Novel and Simple Route to Fabricate 2D Ordered Gold Nanobowl Arrays Based on 3D Colloidal Crystals

ARTICLE *in* LANGMUIR · SEPTEMBER 2011

Impact Factor: 4.46 · DOI: 10.1021/la203158q · Source: PubMed

7 AUTHORS, INCLUDING:

Qin Tao
Southeast University (China)
12 PUBLICATIONS **44** CITATIONS
SEE PROFILE

Jian Dong
Fudan University
108 PUBLICATIONS **1,454** CITATIONS
SEE PROFILE

Langmuir

ARTICLE

pubs.acs.org/Langmuir

Novel and Simple Route to Fabricate 2D Ordered Gold Nanobowl Arrays Based on 3D Colloidal Crystals

Yanying Rao,[†] Qin Tao,[†] Ming An,[‡] Chunhui Rong,[†] Jian Dong,[†] Yurong Dai,[‡] and Weiping Qian*[,†]

[†]State Key Laboratory of Bioelectronics, School of Biological Science and Medical Engineering, Southeast University, Nanjing, 210096, P. R. China

[‡]Department of Physics, Southeast University, Nanjing, 211189, P. R. China

Supporting Information

ABSTRACT: In this study, we present a new method to fabricate large-area two-dimensionally (2D) ordered gold nanobowl arrays based on 3D colloidal crystals by wet chemosynthesis, which combines the advantages of a very simple preparation and an applicability to "real" nanomaterials. By combination of in situ growth of gold nanoshell (GNSs) arrays based on three-dimensional (3D) colloidal silica crystals, a monolayer ordered reversed GNS array (2D ordered GNS array) was conveniently manufactured by an acrylic ester modified biaxial oriented polypropylene (BOPP). 2D ordered gold nanobowl array with adjustable periodic holes, good stability, reproducibility, and repeatability could be obtained when the silica core was etched by HF solution. The surface-enhanced Raman scattering (SERS) enhancement factor (EF) of this 2D ordered gold nanobowl array could reach 1.27×10^7, which shows high SERS enhancing activity and can be used as a universal SERS substrate.

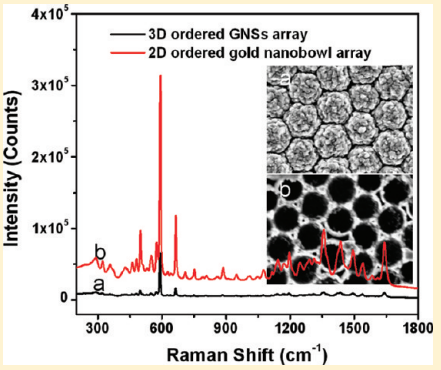

INTRODUCTION

Ordered porous metal materials with well-defined nanostructures have attracted increasing research enthusiasm due to their potential applications in surface-enhanced Raman scattering (SERS),[1] catalysis,[2] optoelectronic and microelectronic devices,[3] biological devices,[4] chemical and biological sensors,[1a,5] and so forth. There are many techniques available for the formation of ordered porous materials, such as electrochemical etching,[6] electron-beam lithography,[7] self-assembly,[8] microcontact printing,[9] and particle-array template methods.[10] A recently reported technique, the colloidal crystals template approach, is very promising for the fabrication of ordered porous metal materials with controlled morphologies by synthesis of three-dimensionally (3D) colloidal crystals and some surface nanostructures.[11] Metal nanomaterials with porous walls have been successfully fabricated by the template method in which sacrificial silica or copolymer spheres are used as template and metal or metal oxide is used to fill up the interspaces or cover the template by nanoparticle depositing.[1] Colloidal template with microscale feature, which is afforded by silica or copolymer spheres, is an excellent platform for creating two-dimensionally (2D) and three-dimensionally (3D) ordered porous metal materials. The metal deposition approach, including codeposition,[8a] electrodeposition,[12] vapor deposition,[13] and chemical deposition,[1] can effectively control the surface morphologies of the ordered porous metal materials.

Noble metal surfaces with ordered porous structured patterns and arrays are of great importance and interest because of their potential applications in the fabrication of chemical and biological sensors based on SERS or surface plasmon resonance (SPR).[1a] Metals such as silver and gold are among the best materials for SERS substrates.[14] Gold, due to its strong biocompatibility, stability, nonbiotoxicity, and superior optical properties, shows superiority in biosensor and SERS performances.[15] Gold ordered nanobowl/nanohole arrays fabricated by in situ chemical deposition with long-range periodic bowl-like shape and controlled diameter of the bowl opening, which can greatly improve its application in SERS and SPR sensing, have attracted great interest among the ordered porous metal materials. However, cheap, efficient and convenient method of fabrication is rarely reported.

Herein, we report a novel method to fabricate large-area 2D ordered gold nanobowl arrays with adjustable periodic holes, good stability, reproducibility, and repeatability via in situ growth gold nanoshells (GNSs) on the surface of SiO_2 colloidal crystals by wet chemosynthesis, and then effectively reversed the GNSs with a monolayer (2D) array by an acrylic ester modified biaxial oriented polypropylene (BOPP). A 2D ordered gold nanobowl array that attached on the BOPP could be obtained when the silica core was etched by HF solution. The method presented here is convenient, cost-effective, and productive. Moreover, due to the long-range periodic porous structures and the higher surface area, the 2D ordered gold nanobowl arrays show high SERS enhancement and can be used as universal SERS substrates.

Received: August 12, 2011
Revised: September 16, 2011
Published: September 20, 2011

EXPERIMENTAL SECTION

Materials and Reagents. Silica colloidal spheres (~110, 180, and 330 nm) and 3-(aminopropyl)-triethoxysilane (APTES, 98%) were obtained from Nissan Chemical Ind., Ltd., Japan, and Sigma, United States, respectively. Sodium borohydride ($NaBH_4$), hydrogen peroxide (H_2O_2, 30%), chloroauric acid tetrahydrate ($HAuCl_4 \cdot 4H_2O$), potassium carbonate (K_2CO_3), and anhydrous ethanol were bought from Nanjing Sunshine Biotechnology Ltd., China. Niel blue A sulfate (NBA) was purchased from Sigma-Aldrich. All of the chemical reagents were used without further purification, and all of them were analytical grade. The acrylic ester modified biaxially oriented polypropylene (BOPP) was bought from Deli Ltd., China (pressure sensitive adhesive transparent tap). $K_2CO_3/HAuCl_4$ solution (growth solution) was prepared as follows:[16] 400 mL aqueous K_2CO_3 solution (0.25 mg mL^{-1}) was mixed with 6 mL $HAuCl_4$ (1%) stock solution under continuous stirring for 20 min and aged in the dark at 4 °C for 4 days. The aqueous solution used in the experiments was prepared by Milli-Q water from Milli-Q system (resistivity >18 MΩ).

Fabrication and Self-Assembly of APTES-Functionalized Silica Colloidal Sphere Templates. First, silica colloidal sphere templates were purified by centrifuging and redispersing in ethanol at least five times. Then, 0.3 mL APTES was added to 125 mL silica colloidal sphere (~330 nm) suspension (0.056 g mL^{-1} in ethanol). Then, the mixture was vigorously stirred to react at 40 °C overnight; APTES groups will covalently bond to the surfaces of silica spheres, extending their amine groups outward as a new termination of the silica surface.[17] To remove excess reactants from the reaction mixture, the APTES-functionalized silica spheres were purified by centrifuging and redispersing in ethanol at least five times. Then, the amino-functionalized silica spheres were close-packed onto the templates with 3D ordered arrays on glass substrates by the vertical deposition method.[18] The silica crystal templates were dried at room temperature before use.

Synthesis and Adsorption of Gold Nanoparticles (GNPs). GNPs (3−5 nm) were prepared by the reduction of $HAuCl_4$ with $NaBH_4$ according to our previous method:[19] 3 mL $HAuCl_4$ (1%) was added into 200 mL H_2O under vigorous stirring for about 5 min, followed by the addition of 1 mL K_2CO_3 (0.2 M). Then, 9 mL freshly prepared $NaBH_4$ (0.5 mg mL^{-1}) was quickly added to the mixture. The mixture would turn to a wine red color rapidly, which indicated the generation of GNPs. The obtained solution was stored at 4 °C until use. The silica sphere templates were fixed in a beaker containing 40 mL as-prepared GNPs solution (gold seeds) and vigorously stirred for about 6 h.[20] Then, the GNS precursor nanocomposite (SiO_2/GNPs) arrays were rinsed 3 times with Milli-Q water to remove the unattached GNPs and dried in air.

Growth of GNS Array and Fabrication of 2D Ordered Gold Nanobowl Array. To initiate the growth of the attached GNPs, the 2.5 cm × 1.5 cm SiO_2/GNPs arrays were immersed 50 mL $K_2CO_3/HAuCl_4$ solution with the reducing agent H_2O_2 (200 μM) under vigorous stirring at room temperature for 30 min. Then, the GNS arrays were rinsed 3 times with Milli-Q water to remove the growth solution and dried in air. A monolayer of hexagonal close-packed GNS array was lifted up by an acrylic ester modified BOPP from the 3D ordered GNS array. Then, the silica sphere template was removed by 4% hydrofluoric (HF) acid, producing a monolayer ordered gold nanobowl array attached on the acrylic ester modified BOPP. The morphology of GNSs and gold nanobowl arrays at different conditions were characterized by Zeiss ULTRA-plus scanning electron microscope (SEM) at 15 kV.

SERS Measurements. In order to determine the SERS-activity of the GNSs array and gold nanobowl array, all the nanomaterials were soaked in NBA solution (10^{-7} M) for 2 h. The Raman experiments were collected with a Renishaw Invia Reflex system equipped with Peltier-cooled charge-coupled device (CCD) detectors and a Leica microscope.

Scheme 1[a]

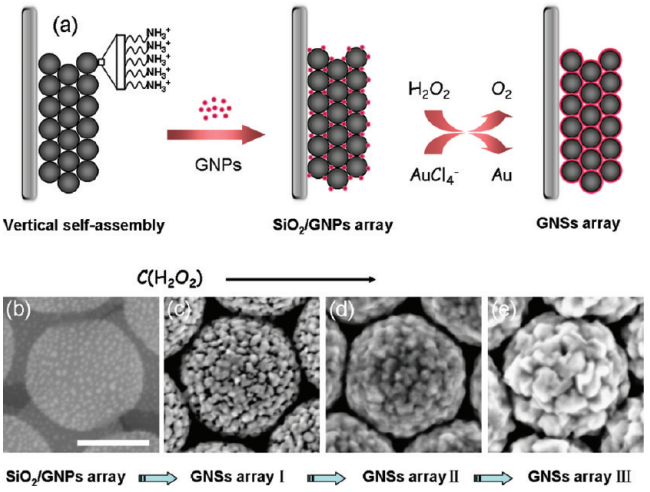

[a] (a) Schematic illustration of the fabrication of H_2O_2-mediated 3D ordered GNS array; SEM images of GNS arrays produced by using SiO_2/GNPs array upon reaction with 40 mL $K_2CO_3/HAuCl_4$ solution and series concentration of H_2O_2. (b) 0 μM, (c) 100 μM, (d) 200 μM, and (e) 300 μM. The scale bar in SEM images is 200 nm.

Samples were excited with a 785 nm diode laser under line-focus mode and the laser power was adjust to 0.05%, which was about 0.06 mW. The corresponding laser was focused onto the sample surface using a 50× long working distance objective. Spectra were collected in continuous mode with 10 s exposure time and accumulated twice and a grating of 1200 mm^{-1} was used. Every SERS spectrum was averaged from 5 measurements. All experiments were performed in triplicate and values were averaged. The microscope should be refocused after every measurement and all Raman experiments were carried out at room temperature (~20 °C).

RESULT AND DISCUSSION

H_2O_2-Mediated Growth of GNSs Arrays. Scheme 1a is the schematic illustration of H_2O_2-mediated growth of ordered GNSs arrays. First, silica spheres were modified with APTES to present the surfaces with positively charged amino groups. Then, the modified spheres formed hexagonal close-packed arrays on glass substrates by the vertical deposition method.[18] Afterward, the silica templates were immersed in a beaker of aqueous GNPs under vigorous stirring. During this process, the negatively charged GNPs would attach onto the amino groups on the modified silica sphere surfaces by electrostatic interactions and SiO_2/GNPs formed.[21] Then, the GNPs that attached on the surface of SiO_2/GNP arrays were used as nucleation sites to template the growth of a gold shell layer by H_2O_2, which is an active reducing agent for the reduction of $AuCl_4^-$ to Au^0. The growth of GNPs was well-controlled by the concentration of H_2O_2 and the amount of $K_2CO_3/HAuCl_4$ solution. With excessive growth solution, the higher the concentration of H_2O_2 used, the more $AuCl_4^-$ will be reduced to Au^0 and deposit onto the GNPs on the surface of SiO_2/GNPs, leading to increases in both the size and the coverage of GNPs until a uniform nanoshell formed, and then, the interspaces among colloidal spheres were filled up as shown in Scheme 1b−e.

The SEM images of Scheme 1b−e show the topography of the SiO_2/GNP arrays in different stages of the shell forming process.

dx.doi.org/10.1021/la203158q |*Langmuir* 2011, 27, 13308–13313

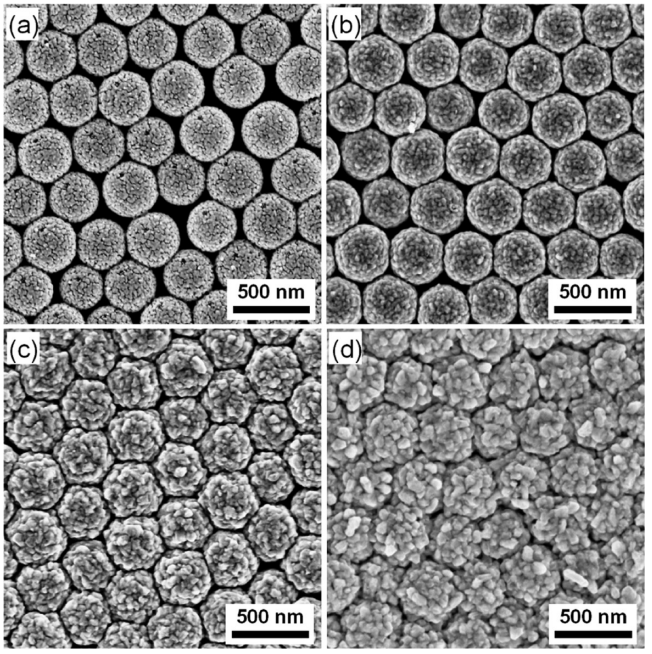

Figure 1. SEM images of GNS arrays produced by using SiO_2/GNPs array upon reaction with 200 μM H_2O_2 and different amount of K_2CO_3/$HAuCl_4$ solution: (a) 30 mL, (b) 40 mL, (c) 50 mL, and (d) 80 mL.

It can be seen that the SiO_2/GNP arrays generated different GNP dimensions and topography under different concentrations of H_2O_2. As shown in Scheme 1b, there were numerous GNPs with diameter around 5 nm attached on the APTES-functionalized silica surface, constituting the SiO_2/GNPs. The interspaces between SiO_2/GNPs were formed by the electronic repulsion effect and steric effect of the APTES. When the reduction process was initiated, the small preadsorbed GNPs would be used as nucleation sites for the subsequent reduction, leading to increases in both the size and the coverage of GNPs on the surface of the silica spheres. With excessive amount of growth solution, more Au will be reduced onto the GNPs under higher concentration of H_2O_2, and the crevices between GNPs become narrower (Scheme 1c) and finally coalesce to form complete GNSs (Scheme 1d). Once the complete GNSs are formed, the additional deposition of gold only increases both the thickness and the roughness of the GNSs (Scheme 1e). Similar results were obtained under 200 μM H_2O_2 and different amount of growth solution (Figure 1). As shown in Figure 1b, the complete GNS arrays with thin shells were formed when 40 mL growth solution was used. Thicker GNSs would be obtained when more growth solution was used (Figure 1c). At the same time, the interspaces between SiO_2/GNPs became narrower and narrower as the shell formed and was finally filled with the reduced gold (Figure 1d).

Fabrication of 2D Ordered Gold Nanobowl Array. Scheme 2 is the schematic illustration of the 2D (monolayer) ordered gold nanobowl array forming process. The GNS array was reversed by an acrylic ester modified BOPP to form a monolayer GNS array (Figure S1, Supporting Information). A monolayer ordered gold nanobowl array attached on the BOPP could be obtained when the silica core was etched by HF solution. A uniform GNS array with appropriate thickness which can be well-controlled by the concentration of H_2O_2 and the amount of K_2CO_3/$HAuCl_4$ solution is crucial to the reversed monolayer GNS array. To obtained a uniform monolayer ordered gold nanobowl array, the most advisible reaction condition is that in which the SiO_2/GNP array reacts with 50 mL K_2CO_3/$HAuCl_4$ solution and 200 μM H_2O_2 for 30 min.

Scheme 2. Schematic Illustration of 2D Ordered Gold Nanobowl Array Forming Process

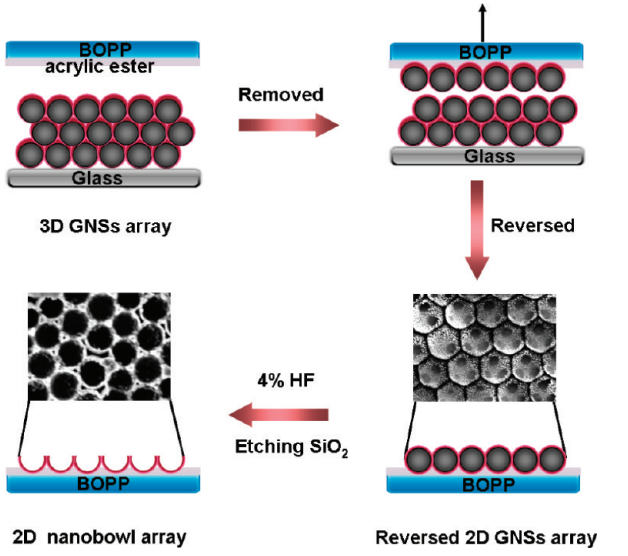

Figure 2 shows the SEM images of the reversed monolayer GNS arrays and ordered gold nanobowl arrays. The 3D ordered GNS array shown in Figure 2a was produced by 200 μM H_2O_2 and 50 mL K_2CO_3/$HAuCl_4$ solution; Figure 2b is the boundary view of the 3D ordered GNS array after being taken off by acrylic ester modified BOPP partly. Figure 2c shows the SEM image of the reversed monolayer GNS array taken from 3D ordered GNS array shown in Figure 2a. As can be seen, the gold coverage on the reverse side of the GNS array was limited. There were numerous GNPs with different sizes attached on the silica surface and the GNPs on the top were smaller than that near the bottom (Figure 2c); this was caused by the concentration gradient of K_2CO_3/$HAuCl_4$ and H_2O_2. The GNSs in the first layer had two diverse sides: the obverse side exposed to the solution was easy to deposit Au^0 (Figure 2a), while for the reverse side connected with the next layer of SiO_2/GNP array, very little growth solution came through this side and less Au^0 was reduced onto it (Figure 2c). The blank spots with no gold deposition were the contact points of two silica layers, indicating that every silica has three contact points with the next silica layer of the hexagonal close-packed array. To prove that the 3D ordered GNS array taken off by the acrylic ester modified BOPP was a monolayer GNS array, an SEM image of the boundary was made, as shown in Figure 2b. Figure 2d–f shows monolayer gold nanobowl arrays with different bore sizes of 330, 180, and 110 nm, respectively. The GNPs on the reversed silica surface shed off once the core was etched by HF solution, and only half-shells, nanobowls, were attached on the BOPP. A uniform GNS array with appropriate thickness which can be well-controlled by the concentration of H_2O_2 and the amount of K_2CO_3/$HAuCl_4$ solution is crucial to the reversed monolayer GNS array and the gold nanobowl array. The gold nanobowl is easy to collapse if the shell is too thin, while an overdose of reduced Au^0 will fill the interspaces between two layers of SiO_2/GNP arrays (produced by using SiO_2/GNP array upon reaction with 200 μM H_2O_2 and 80 mL K_2CO_3/$HAuCl_4$ solution), resulting in a fast connection

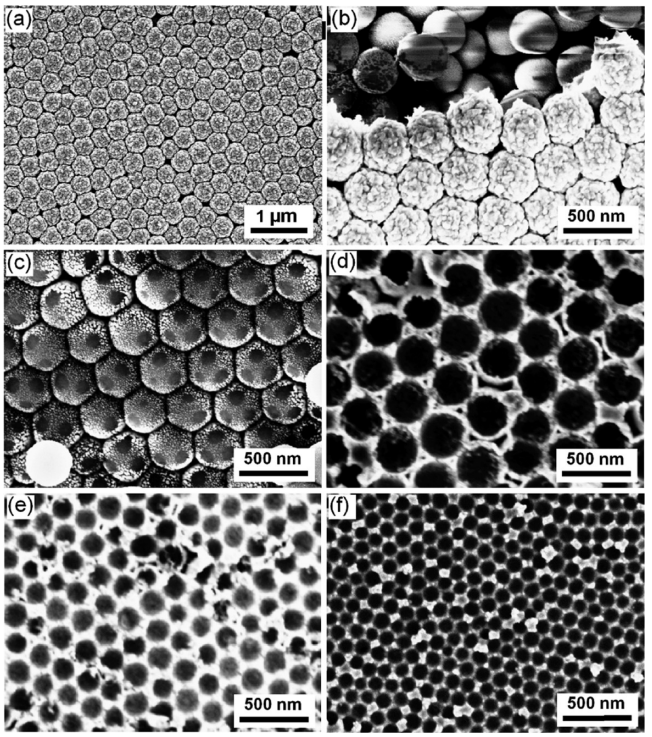

Figure 2. SEM images of (a) 3D ordered GNS array produced by using SiO_2/GNP arrays upon reaction with 200 μM H_2O_2 and 50 mL K_2CO_3/$HAuCl_4$ solution, (b) the boundary view of the 3D ordered GNS array after being taken off by acrylic ester modified BOPP partly, (c) the reversed monolayer GNS array that attached on the acrylic ester modified BOPP and 2D ordered gold nanobowl arrays with different bore sizes of (d) 330 nm, (e) 180 nm, and (f) 110 nm.

of them, and reversed GNS arrays would no longer be monolayer (Figure S2, Supporting Information).

In the formation process of reversed monolayer GNS arrays, there exist three kinds of forces: the force between the adhesive acrylic ester and the GNS array in the first layer (F1), the force between the GNS arrays in the first layer and second layer (F2), and the force between the GNS arrays in the second layer and third layer (F3). When F1 > F2, and F3 > F2 or F3 is lower than the gravity of the second layer array, the reversed monolayer GNS array formed (Scheme 2). In fact, a monolayer gold nanobowl array would be obtained no matter whether the reversed GNS was monolayer or multilayer if the concentration of H_2O_2 and the amount of K_2CO_3/$HAuCl_4$ solution was appropriate. The reason is that most of the Au^0 was reduced onto the obverse side of the first layer of the SiO_2/GNPs array. There were only some small GNPs on the reverse side or the next layer of SiO_2/GNPs array, which will shed off once the silica core was etched by HF solution. The method exhibited versatility in the fabrication of the monolayer ordered gold nanobowl with different bore size. By varying the shell thickness and the core diameter, the bore size of the gold nanobowl could be readily adjusted.

SERS Properties. Since it was discovered in the late 1970s,[22] SERS has been used in a wide range of fields such as trace detection,[23] clinical diagnosis,[24] chemical and biochemical monitoring,[25] and so forth. However, all of the SERS applications depend on the substrate with SERS-active structures. Benefiting from the development of nanoscience and especially

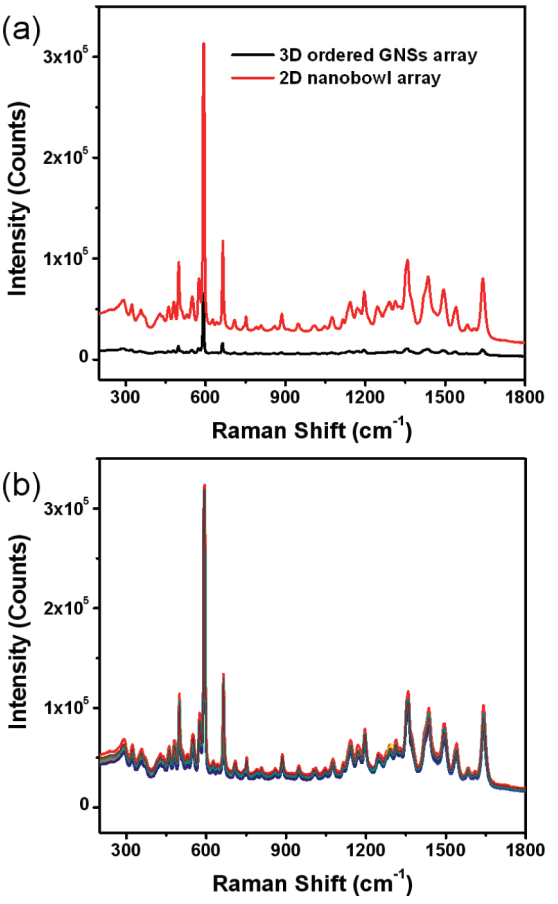

Figure 3. (a) SERS spectra of 10^{-7} M NBA on 3D ordered GNSs array and 2D ordered gold nanobowl array (with a core diameter of 330 nm) substrates, respectively. (b) 12 SERS spectra taken from 12 random spots on a gold nanobowl array.

nanofabrication, SERS substrates with well-defined architectures and high reproducibility can be made.[26]

Both the obtained 3D ordered GNSs arrays and 2D ordered gold nanobowl arrays were predicted to show high performance when they were used as SERS substrates. In order to demonstrate the SERS activity of 3D GNS arrays and 2D gold nanobowl arrays, NBA was chosen as a Raman report molecule. The as-prepared GNSs or gold nanobowl arrays were immersed in 10^{-7} M NBA solution before the Raman experiments. Figure 3a shows the SERS spectra of NBA on the 3D ordered GNS array and 2D ordered gold nanobowl array substrates as shown in Figure 1c (with a core of 330 nm) and Figure 2b (with a bore size of 330 nm). The spectra present the characteristic Raman shifts of NBA at 592 cm^{-1} and 1638 cm^{-1}, whose modes were formed by the positively charged nitrogen and had high specificity.[27] As can be seen, the SERS signal of 2D ordered gold nanobowl array was ~5 times that of the corresponding 3D ordered GNS array (Figure 3a). Supporting Information Figure S3 shows SERS intensity of 10^{-7} M NBA on 3D ordered GNS array and the corresponding 2D ordered gold nanobowl array substrates with different diameters of the silica core (110 nm, 180 nm 330 nm), respectively. The results indicated that the nanobowl array had a stronger SERS enhancement than the corresponding GNS array (the bore size of the nanobowl equals the core diameter of GNSs), which has been confirmed by the experiment results of

dx.doi.org/10.1021/la203158q |*Langmuir* 2011, 27, 13308–13313

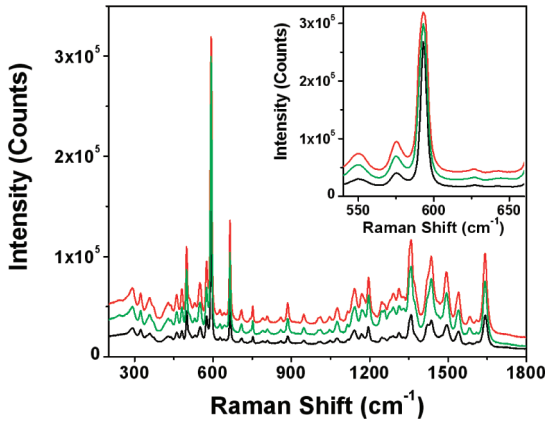

Figure 4. SERS spectra of 10^{-7} M NBA on 2D gold nanobowl array (with a core diameter of 330 nm) substrates from 3 batches. Inset spectra are the 592 band of NBA from 3 batches.

Wang et al.[13c] This is because, first, many crevices on the nanobowl or between nanobowls were created during the HF etching process (the gold shell shrunk slightly when the silica core was etched), which is particularly desirable for the SERS effect; second, the excitation laser was absorbed more effectively by the nanobowl (concave surface) than the nanoshell (convex surface) and so did the collection of Raman scattering signal.

The SERS enhancement factor (EF) is calculated by using the averaged surface EF (ASEF; also named SERS substrate EF, SSEF; as shown in Supporting Information).[1a,28] The ASEF value of the 2D ordered gold nanobowl array and 3D ordered GNS array substrates produced with the diameter of 110, 180, and 330 nm silica core were estimated (Table S1, Supporting Information). The results showed that the ASEF value of 2D ordered gold nanobowl arrays with the diameter of 330 nm silica cores is 1.27×10^7. The results confirm that the 2D ordered gold nanobowl arrays have super SERS enhancement compared with the corresponding 3D ordered GNSs arrays.

For an ideal SERS substrate, it must be uniform and with high reproducibility and repeatability.[26b] Figure 3b shows the 12 SERS spectra taken from 12 random spots on a gold nanobowl array as shown in Figure 2b. As can be seen, the variation of SERS intensity from different spots of the same array was slight, which shows that the gold nanobowl array has good reproducibility as a SERS substrate. The batch to batch variation of SERS intensity from three different arrays as shown in Figure 4 indicated that the gold nanobowl array had good repeatability.

The 2D ordered gold nanobowl arrays show high SERS enhancement and can be used as the candidate structures for SERS sensors as they have several advantages: first, they could be uniformly and controllably manufactured on the colloidal crystal templates; second, a large area of ordered periodic metal nanobowl structures with homogeneous, stable, and controllable bore size can be generated and the nanobowl gives the structure higher surface area; third, the spectra acquired from ordered substrates show better reproducibility and less variation compared to the disordered substrates according to multivariate analysis; finally, the 2D ordered gold nanobowl arrays attached on the acrylic ester modified BOPP are much more stable than that attached on a glass substrate.

CONCLUSIONS

In summary, this work presents a novel in situ growth of GNSs based on a 3D colloidal silica crystal technique for fabricating large-area 2D ordered gold nanobowl arrays with adjustable periodic holes and good stability. First, regular arrayed GNSs were prepared with high structural controllability by using in situ growth GNSs on the SiO_2 colloidal crystals templates; then, a monolayer ordered reversed GNS array was conveniently fabricated by an acrylic ester modified BOPP; finally, 2D ordered gold nanobowl arrays attached on the BOPP could be obtained when the silica core was etched by HF solution. Furthermore, the sensitivity growth gold nanobowl arrays with controlled pore size show high SERS activity which can be used as excellent SERS sensors. Catalysis, biosensors, and chemical sensors could also be constructed by using our strategy based on the SERS or SPR properties. This method is convenient, cost-effective, and productive, and has the potential for being a practical route to construct porous-film-related nanostructured devices in the near future. To the best of our knowledge, this is the first report on using acrylic ester modified BOPP instead of glass or silicon wafer as substrate to hold GNS array or gold nanobowl array.

ASSOCIATED CONTENT

Supporting Information. Additional figures and data as described in the text. This material is available free of charge via the Internet at http://pubs.acs.org.

AUTHOR INFORMATION

Corresponding Author

*Tel./fax: +862583795719. E-mail: wqian@seu.edu.cn.

ACKNOWLEDGMENT

We gratefully acknowledge support from the Chinese 973 Project (grants: 2012CB933302 and 2010CB933902) and National Natural Science Foundation of China (grants: 21175022 and 90923010).

REFERENCES

(1) (a) Hong, G. S.; Li, C.; Qi, L. M. *Adv. Funct. Mater.* **2010**, *20*, 3774–3783. (b) Lu, L. H.; Capek, R.; Kornowski, A.; Gaponik, N.; Eychmuller, A. *Angew. Chem., Int. Ed.* **2005**, *44*, 5997–6001. (c) Lu, L. H.; Eychmuller, A.; Kobayashi, A.; Hirano, Y.; Yoshida, K.; Kikkawa, Y.; Tawa, K.; Ozaki, Y. *Langmuir* **2006**, *22*, 2605–2609.

(2) (a) Chai, G. S.; Shin, I. S.; Yu, J. S. *Adv. Mater.* **2004**, *16*, 2057–+. (b) Kim, S. W.; Kim, M.; Lee, W. Y.; Hyeon, T. *J. Am. Chem. Soc.* **2002**, *124*, 7642–7643.

(3) Veinot, J. G. C.; Yan, H.; Smith, S. M.; Cui, J.; Huang, Q. L.; Marks, T. J. *Nano Lett.* **2002**, *2*, 333–335.

(4) Dersch, R.; Steinhart, M.; Boudriot, U.; Greiner, A.; Wendorff, J. H. *Polym. Adv. Technol.* **2005**, *16*, 276–282.

(5) Jia, L. C.; Cai, W. P. *Adv. Funct. Mater.* **2010**, *20*, 3765–3773.

(6) Chiappini, C.; Tasciotti, E.; Fakhoury, J. R.; Fine, D.; Pullan, L.; Wang, Y. C.; Fu, L. F.; Liu, X. W.; Ferrari, M. *ChemPhysChem* **2010**, *11*, 1029–1035.

(7) Ebbesen, T. W.; Lezec, H. J.; Ghaemi, H. F.; Thio, T.; Wolff, P. A. *Nature* **1998**, *391*, 667–669.

(8) (a) Chen, Y. W.; Kang, E. T.; Neoh, K. G.; Greiner, A. *Adv. Funct. Mater.* **2005**, *15*, 113–117. (b) Shah, P. S.; Sigman, M. B.; Stowell, C. A.; Lim, K. T.; Johnston, K. P.; Korgel, B. A. *Adv. Mater.* **2003**, *15*, 971–974.

(9) Xia, Y. N.; Rogers, J. A.; Paul, K. E.; Whitesides, G. M. *Chem. Rev.* **1999**, *99*, 1823–1848.
(10) Haupt, M.; Miller, S.; Glass, R.; Arnold, M.; Sauer, R.; Thonke, K.; Moller, M.; Spatz, J. P. *Adv. Mater.* **2003**, *15*, 829–831.
(11) Jiang, P.; Bertone, J. F.; Colvin, V. L. *Science* **2001**, *291*, 453–457.
(12) Sun, F. Q.; Cai, W. P.; Li, Y.; Cao, B. Q.; Lu, F.; Duan, G. T.; Zhang, L. D. *Adv. Mater.* **2004**, *16*, 1116–1121.
(13) (a) Zhang, X. Y.; Yonzon, C. R.; Van Duyne, R. P. *J. Mater. Res.* **2006**, *21*, 1083–1092. (b) Li, Y. Y.; Pan, J.; Zhan, P.; Zhu, S. N.; Ming, N. B.; Wang, Z. L.; Han, W. D.; Jiang, X. Y.; Zi, J. *Opt. Express* **2010**, *18*, 3546–3555. (c) Chen, L.; Liu, F. X.; Zhan, P.; Pan, J.; Wang, Z. L. *Chin. Phys. Lett.* **2011**, *28*, 057801.
(14) (a) Wang, W.; Li, Z. P.; Gu, B. H.; Zhang, Z. Y.; Xu, H. X. *ACS Nano* **2009**, *3*, 3493–3496. (b) Lu, L.; Eychmuller, A. *Acc. Chem. Res.* **2008**, *41*, 244–253. (c) Wang, H. H.; Liu, C. Y.; Wu, S. B.; Liu, N. W.; Peng, C. Y.; Chan, T. H.; Hsu, C. F.; Wang, J. K.; Wang, Y. L. *Adv. Mater.* **2006**, *18*, 491–495.
(15) Alvarez-Puebla, R. A.; Ross, D. J.; Nazri, G. A.; Aroca, R. F. *Langmuir* **2005**, *21*, 10504–10508.
(16) Wang, Y.; Qian, W. P.; Tan, Y.; Ding, S. H. *Biosens. Bioelectron.* **2008**, *23*, 1166–1170.
(17) Rao, Y. Y.; Chen, Q. F.; Dong, J. A.; Qian, W. P. *Analyst* **2011**, *136*, 769–774.
(18) Qian, W. P.; Gu, Z. Z.; Fujishima, A.; Sato, O. *Langmuir* **2002**, *18*, 4526–4529.
(19) Li, H.; Ma, X. Y.; Dong, J.; Qian, W. P. *Anal. Chem.* **2009**, *81*, 8916–8922.
(20) (a) Wang, Y.; Qian, W. P.; Tan, Y.; Ding, S. H.; Zhang, H. Q. *Talanta* **2007**, *72*, 1134–1140. (b) Ding, S. H.; Qian, W. P.; Tan, Y.; Wang, Y. *Langmuir* **2006**, *22*, 7105–7108.
(21) Oldenburg, S. J.; Averitt, R. D.; Westcott, S. L.; Halas, N. J. *Chem. Phys. Lett.* **1998**, *288*, 243–247.
(22) (a) Fleischm., M; Hendra, P. J.; Mcquilla, Aj *Chem. Phys. Lett.* **1974**, *26*, 163–166. (b) Albrecht, M. G.; Creighton, J. A. *J. Am. Chem. Soc.* **1977**, *99*, 5215–5217.
(23) Nie, S. M.; Emery, S. R. *Science* **1997**, *275*, 1102–1106.
(24) (a) Qian, X. M.; Peng, X. H.; Ansari, D. O.; Yin-Goen, Q.; Chen, G. Z.; Shin, D. M.; Yang, L.; Young, A. N.; Wang, M. D.; Nie, S. M. *Nat. Biotechnol.* **2008**, *26*, 83–90. (b) Culha, M.; Stokes, D.; Allain, L. R.; Vo-Dinh, T. *Anal. Chem.* **2003**, *75*, 6196–6201.
(25) (a) Dijkstra, R. J.; Scheenen, W. J. J. M.; Dam, N.; Roubos, E. W.; ter Meulen, J. J. *J. Neurosci. Methods* **2007**, *159*, 43–50. (b) Levin, C. S.; Janesko, B. G.; Bardhan, R.; Scuseria, G. E.; Hartgerink, J. D.; Halas, N. J. *Nano Lett.* **2006**, *6*, 2617–2621. (c) Ko, H.; Singamaneni, S.; Tsukruk, V. V. *Small* **2008**, *4*, 1576–1599.
(26) (a) Lin, X. M.; Cui, Y.; Xu, Y. H.; Ren, B.; Tian, Z. Q. *Anal. Bioanal. Chem.* **2009**, *394*, 1729–1745. (b) Natan, M. J. *Faraday Discuss.* **2006**, *132*, 321–328.
(27) do Nascimento, G. M.; Temperini, M. L. A. *J. Raman Spectrosc.* **2008**, *39*, 772–778.
(28) (a) Le Ru, E. C.; Blackie, E.; Meyer, M.; Etchegoin, P. G. *J. Phys. Chem. C* **2007**, *111*, 13794–13803. (b) Kim, K.; Yoon, J. K. *J. Phys. Chem. B* **2005**, *109*, 20731–20736. (c) Dong, S. J.; Wang, Y. L.; Chen, H. J.; Wang, E. K. *J. Chem. Phys.* **2006**, *125*, 044710.